Developing Wireless Power Transfer For Electric Vehicle Applications

S.ugendran[1], S.chandhruprakash[2], S.shanmuganathan[3], A.sudeep[4], M.Sivakumar[5]
[1, 2, 3, 4] Dept of ECE
[5]Assistance Professor Dept of ECE
[1, 2, 3, 4, 5] NSN COLLEGE OF ENGINEERING AND TECHNOLOGY

Abstract- *Wireless power transfer (WPT) using magnetic resonance is the technology which could set human free from the annoying wires. In fact, the WPT adopts the same basic theory which has already been developed for at least 30 years with the term inductive power transfer. WPT technology is developing rapidly in recent years. At kilowatts power level, the transfer distance increases from several millimeters to several hundred millimeters with a grid to load efficiency above 90%. The advances make the WPT very attractive to the electric vehicle (EV) charging applications in both stationary and dynamic charging scenarios. This paper reviewed the technologies in the WPT area applicable to EV wireless charging. By introducing WPT in EVs, the obstacles of charging time, range, and cost can be easily mitigated. Battery technology is no longer relevant in the mass market penetration of EVs. It is hoped that researchers could be encouraged by the state-of-the-art achievements, and push forward the further development of WPT as well as the expansion of EV.*

Keywords- Dynamic charging, electric vehicle (EV), inductive power transfer (IPT), safety guidelines, stationary charging, wireless power transfer (WPT).

I. INTRODUCTION

FOR energy, environment, and many other reasons, the electrification for transportation has been carrying out for many years. In railway systems, the electric locomotives have already been well developed for many years. A train runs on a fixed track. It is easy to get electric power from a conductor rail using pantograph sliders. However, for electric vehicles (EVs), the high flexibility makes it not easy to get power in a similar way. Instead, a high power and large capacity battery pack is usually equipped as an energy storage unit to make an EV to operate for a satisfactory distance.

Until now, the EVs are not so attractive to consumers even with many government incentive programs. Government subsidy and tax incentives are one key to increase the market share of EV today. The problem for an electric vehicle is nothing else but the electricity storage technology, which requires a battery which is the bottleneck today due to its unsatisfactory energy density, limited life time and high cost.

In an EV, the battery is not so easy to design because of the following requirements: high energy density, high power density, affordable cost, long cycle life time, good safety, and reliability, should be met simultaneously. Lithium-ion batteries are recognized as the most competitive solution to be used in electric vehicles [1]. However, the energy density of the commercialized lithium-ion battery in EVs is only 90–100 Wh/kg for a finished pack [2].[1]This number is so poor compared with gasoline, which has an energy density about 12000 Wh/kg. To challenge the 300-mile range of an internal combustion engine power vehicle, a pure EV needs a large amount of batteries which are too heavy and too expensive. The lithium-ion battery cost is about 500$/kWh at the present time. Considering the vehicle initial investment, maintenance, and energy cost, the owning of a battery electric vehicle will make the consumer spend an extra 1000$/year on average compared with a gasoline-powered vehicle [1]. Besides the cost issue, the long charging time of EV batteries also makes the EV not acceptable to many drivers. For a single charge, it takes about one half-hour to several hours depending on the power level of the attached charger, which is many times longer than the gasoline refueling process. The EVs cannot get ready immediately if they have run out of battery energy. To overcome this, what the owners would most likely do is to find any possible opportunity to plug-in and charge the battery. It really brings some trouble as people may forget to plug-in and find themselves out of battery energy later on. The charging cables on the floor may bring tripping hazards. Leakage from cracked old cable, in particular in cold zones, can bring additional hazardous conditions to the owner. Also, people may have to brave the wind, rain, ice, or snow to plugin with the risk of an electric shock.
The wireless power transfer (WPT) technology, which can eliminate all the charging troublesome, is desirable by the EV

[1] Although lithium ion battery can achieve up to 200 Wh/kg for individual cells, the battery pack requires structure design, cooling, and battery management systems. The over energy density of a battery pack is much lower than the cell density.

owners. By wirelessly transferring energy to the EV, the charging becomes the easiest task. For a stationary WPT system, the drivers just need to park their car and leave. For a dynamic WPT system, which means the EV could be powered while driving; the EV is possible to run forever without a stop. Also, the battery capacity of EVs with wireless charging could be reduced to 20% or less compared to EVs with conductive charging.

Although the market demand is huge, people were just wondering whether the WPT could be realized efficiently at a reasonable cost. The research team from MIT published a paper in Science [3], in which 60 W power is transferred at a 2-m distance with the so called strongly coupled magnetic resonance theory. The result surprised the academia and the WPT quickly became a hot research area. A lot of interesting works were accomplished with different kinds of innovative circuit, as well as the system analysis and control [4]–[9]. The power transfer path can even be guided using the domino-form repeaters [10], [11]. In order to transfer power more efficiently and further, the resonant frequency is usually selected at MHz level, and air-core coils are adopted.

When the WPT is used in the EV charging, the MHz frequency operation is hard to meet the power and efficiency criteria. It is inefficient to convert a few to a few hundred kilowatts power at MHz frequency level using state-of-theart power electronics devices. Moreover, air-core coils are too sensitive to the surrounding ferromagnetic objects. When an air-core coil is attached to a car, the magnetic flux will go inside the chassis causing high eddy current loss as well as a significant change in the coil parameters. To make it more practical in the EV charging, ferrite as a magnetic flux guide and aluminum plate as a shield are usually adopted in the coil design [12]. With the lowered frequency to less than 100 kHz, and the use of ferrite, the WPT system is no different from the inductive power transfer (IPT) technology which has been developed for many years [13]–[39]. In fact, since the WPT is based on the nonradiative and near-field electromagnetic, there is no difference with the traditional IPT which is based on magnetic field coupling between the transmitting and receiving coils. The IPT system has already been proposed and applied to various applications, such as underwater vehicles [32]–[34], mining systems [16], cordless robots in automation production lines [36]–[39], as well as the charging of electric vehicles [13], [14], [25]–[27].

Recently, as the need of EV charging and also the progress in technology, the power transfer distance increases from several millimeters to a few hundred millimeters at kilowatts power level [12], [14], [40]–[60]. As a proof-of-concept of a roadway inductively powered EV, the Partners for Advance Transit and Highways (PATH) program was conducted at the UC Berkeley in the late 1970s [14], [54]. A 60 kW, 35-passanger bus was tested along a 213 m long track with two powered sections. The bipolar primary track was supplied with 1200 A, 400 Hz ac current. The distance of the pickup from the primary track was 7.6 cm. The attained efficiency was around 60% due to limited semiconductor technology. During the last 15 years, researchers at Auckland University have focused on the inductive power supply of movable objects. Their recent achievement in designing pads for the stationary charging of EV is worth noting. A 766 mm × 578 mm pad that delivers 5 kW of power with over 90% efficiency for distances about 200 mm was reported [48], [55]. The achieved lateral and longitudinal misalignment tolerance is 250 and 150 mm, respectively. The knowledge gained from the on-line electric vehicle (OLEV) project conducted at the Korea Advanced Institute of Science and Technology (KAIST) also contributes to the WPT design. Three generations of OLEV systems have been built: a light golf cart as the first

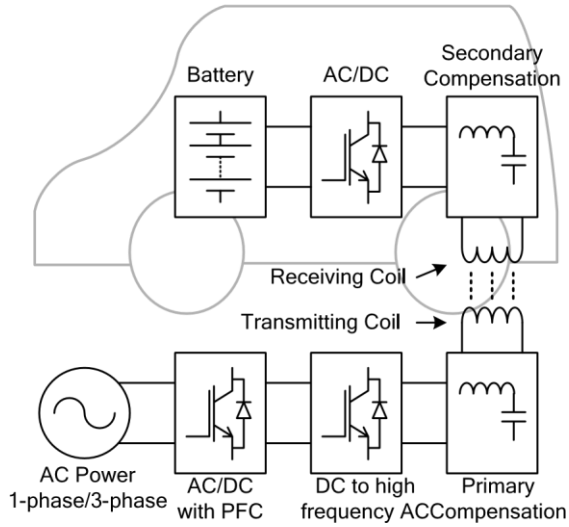

Fig. 1. Typical wireless EV charging system.

generation, a bus for the second, and an SUV for the third.

The accomplishment of the second and the third is noteworthy: 60 kW power transfer for the buses and 20 kW for theSUVs with efficiency of 70% and 83%, respectively; allowable vertical distance and lateral misalignment up to 160 mm and up to 200 mm, respectively [56], [57]. In the United States, more and more public attention was drawn to the WPT since the publication of the 2007 Science paper [3]. The WiTricity Corporation with technology from MIT released their WiT3300 development kit, which achieves 90% efficiency over a 180 mm gap at 3.3 kW output. Recently, a wireless charging system prototype for EV was developed at Oak Ridge National Laboratory (ORNL) in the United States.

The tested efficiency is nearly 90% for 3 kW power delivery [53]. The research at the University of Michigan–Dearborn achieved a 200 mm distance, 8 kW WPT system with dc to dc efficiency as high as 95.7% [61]. From the functional aspects, it could be seen that the WPT for EV is ready in both stationary and dynamic applications. However, to make it available for large-scale commercialization, there is still abundant work to be done on the performance optimization, setup of the industrial standards, making it more cost effective, and so on.

This paper starts with the basic WPT theory, and then gives a brief overview of the main parts in a WPT system, including the magnetic coupler, compensation network, power electronics converter, study methodology, and its control, and some other issues like the safety considerations. By introducing the latest achievements in the WPT area, we hope the WPT in EV applications could gain a widespread acceptance in both theoretical and practical terms. Also, we hope more researchers could have an interest and make more brilliant contributions in the developing of WPT technology.

II. FUNDAMENTAL THEORY

A typical wireless EV charging system is shown in Fig. 1. It includes several stages to charge an EV wirelessly. First, the utility ac power is converted to a dc power source by an ac to dc converter with power factor correction.

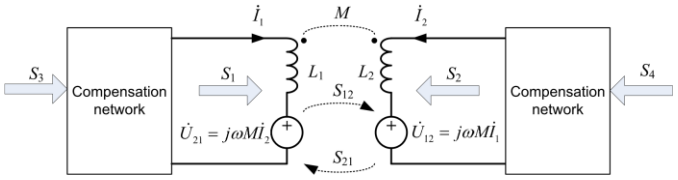

Fig. 2. General two-coil WPT system.

Then, the dc power is converted to a high-frequency ac to drive the transmitting coil through a compensation network. Considering the insulation failure of the primary side coil, a high-frequency isolated transformer may be inserted between the dc-ac inverter and primary side coil for extra safety and protection. The high-frequency current in the transmitting coil generates an alternating magnetic field, which induces an ac voltage on the receiving coil. By resonating with the secondary compensation network, the transferred power and efficiency are significantly improved. At last, the ac power is rectified to charge the battery. Fig. 1 shows that a wireless EV charger consists of the following main parts:

1) the detached (or separated, loosely coupled) transmitting and receiving coils. Usually, the coils are built with ferrite and shielding structure, in the later sections, the term magnetic coupler is used to represent the entirety, including coil, ferrite, and shielding;
2) the compensation network; 3) the power electronics converters.

The main difference between a wireless charger and a conventional conductive or wired charger is that a transformer is replaced by a set of loosely couple coils. To give a quick idea of the WPT principle, the coil and the compensation network are pulled out separately, as shown in Fig. 2, where L_1 represents the self-inductance of the primary side transmitting coil and L_2 represents the self-inductance of the receiving coil; $I\dot{}1$ and $I\dot{}2$ are the current in the two coils; $U\dot{}12$ is the voltage in the secondary coil that is induced by the current in the primary side coil. $U\dot{}21$ is the voltage in the primary coil that is induced by the current in secondary side coil due to coupling, or mutual inductance between the primary and secondary coils. S_1 and S_2 are the apparent power goes into L_1 and L_2, respectively. S_3 and S_4 are the apparent power provided by the power converter. S_{12} and S_{21} represent the apparent power exchange between the two coils. The form of the compensation network is not specified. The characteristics of the compensation network will be discussed later.

As shown in Fig. 2, neglecting the coil resistance and magnetic losses, we can calculate the simplified form of exchanged complex power from L_1 to L_2

$$S\dot{}12 = -\dot{U}_{12}\dot{I}_2^* = -j\omega M\dot{I}_1\dot{I}_2^*$$
$$= \omega MI_1I_2\sin\phi_{12} - j\omega MI_1I_2\cos\phi_{12} \quad (1)$$
$$S\dot{}21 = -\dot{U}_{21}\dot{I}_1^* = -j\omega M\dot{I}_2\dot{I}_1^*$$
$$= -\omega MI_1I_2\sin\phi_{12} - j\omega MI_1I_2\cos\phi_{12} \quad (2)$$

where I_1 and I_2 are the root mean square value and ϕ_{12} is the phase difference between $I\dot{}1$ and $I\dot{}2$. The active power transfer from the primary side to the secondary side can be expressed as

$$P_{12} = \omega MI_1I_2\sin\phi_{12}. \quad (3)$$

The system shown in Fig. 2 can transfer active power in both directions. In the analysis below, we assume the power is transferred from L_1 to L_2. When $\phi_{12} = \pi/2$, which means $I\dot{}1$ leads $I\dot{}2$ by a quarter cycle, the maximum power can be transferred from L_1 to L_2.

The total complex power goes into the two-coil system is $\dot{S} =$

$$= j\left(\omega L_1 \dot{I}_1 + \omega M \dot{I}_2\right)\dot{I}_1^* + j\left(\omega L_2 \dot{I}_2 + \omega M \dot{I}_1\right)\dot{I}_2^*$$
$$= j\omega\left(L_1 I_1^2 + L_2 I_2^2 + 2M I_1 I_2 \cos\varphi_{12}\right). \quad (4)$$
$$\dot{S}1 + \dot{S}2$$

Therefore, the total reactive power goes into the two-coil system is

$$Q = \omega L_1 I_1^2 + L_2 I_2^2 + 2MI_1 I_2 \cos\phi_{12}. \quad (5)$$

For a traditional transformer, the reactive power represents the magnetizing power. Higher magnetizing power brings higher copper and core loss. To increase the transformer efficiency, the ratio between the active power and reactive power should be maximized. The ratio is defined by *f* *(ϕ*12*)* =

$||PQ_{12}||$ =

$\omega L_1 I \omega M I^1 I^2 \sin \phi M I^{12} {}_1 I_2 \cos\Phi_{12}$

${}_1^2 + \omega L_2 I_2^2 + 2\omega$

= ${}_2\,{}_2 k 1 - \cos_1 {}^2 \phi_{12}$ = + $1 + \cos^2 \phi_{12}$ $\frac{k}{x}$ + $+2k$ $2k\cos\phi$

$\cos\phi 21\; x\; 1\; 12$

(6)

where $\pi/2 < \phi_{12} < \pi$

$$x = \frac{L_1 I_1}{L_2 I_2} > 0$$

k is the coupling coefficient between L_1 and L_2.

To achieve the maximum value of f (ϕ_{12}), we solve the following equations:

$$\frac{\partial}{\partial\phi 12} f(\phi 12) = 0, \qquad \frac{\partial^2}{\partial^2\phi 12} f(\phi 12) < 0 \qquad (7)$$

and the solutions are

$\cos\phi 12 = -$ x $2+k$ $1x$, $\sin\phi^{12} =$ 1 $-$ $_x$ $4+k21x$ 2 . (8)

When k is close to 1, it is a traditional transformer. In this case, if $\dot{I}2$ is an induced current by $\dot{I}1$, x will be close to 1. Thus, $\cos\phi_{12} \approx -1$. The phase difference between $\dot{I}1$ and $\dot{I}2$ is nearly 180°. While for WPT, k is close to 0. f (ϕ_{12}) is maximized at $\sin\phi_{12} = 1$, at which point the transferred power is also maximized. The phase between $\dot{I}1$ and $\dot{I}2$ is around 90° instead of 180°. Hence we can see the difference between the tightly and the loosely coupled coils.

The degree of coupling affects the design of the compensation network. Taking the series–series topology as an example, there are two ways to design the resonant capacitor. One way is design the capacitor to resonate with the leakage inductance [46], [62] which could achieve a higher f (ϕ_{12}). Another way is to resonate with the coil self-inductance [27], [41], [63] which could maximum the transferred power at a certain coil current. When the coupling is tight with a ferrite, like $k > 0.5$, it is important to increase f (ϕ_{12}) to achieve better efficiency. In this case, resonate with the coil self inductance, which makes $\phi_{12} = \pi/2$ and lowers f (ϕ_{12}), is not recommended. Otherwise the magnetizing loss may significantly increase. When the capacitor resonates with the leakage inductance, it is like the leakage inductance is compensated. This makes the transformer perform as a traditional one and increases f (ϕ_{12}). However, the overall system does not work at a resonant mode. When the coupling is loose, like $k < 0.5$, which is the case for the EV wireless charging, usually the capacitor is tuned with the self inductance to make the system working at a resonate mode to achieve maximum transferred power at a certain coil current. In this case, most of the magnetic field energy is stored in the large air gap between the two coils. The hysteresis loss in the ferrite is not so relative to the magnetizing power. However, the loss in the copper wire is proportional to the square of the conducting current. To efficiently transfer more power at a certain coil current, the induced current $\dot{I}2$ should lag $\dot{I}1$ by 90°. Since the induced voltage $\dot{U}12$ on the receiving coil lags $\dot{I}1$ by 90°, $\dot{U}12$ and $\dot{I}2$ should be in phase. The secondary side should have a pure resistive characteristic seen from $\dot{U}12$ at the frequency of $\dot{I}1$. At the meanwhile, the primary side input apparent power S_3 should be minimized. At $\cos\phi_{12} = 0$, the complex power $\dot{S}1$ is

$$\dot{S}1 = j\omega L_1 I_1^2 + \omega M I_1 I_2. \qquad (9)$$

Ideally, the primary side compensation network should cancel the reactive power and make $S_3 = \omega_0 M I_1 I_2$, where ω_0 is the resonant frequency. From the above analysis, we see for a certain transferred power, it is necessary to make the secondary side resonant to reduce the coil volt-ampere (VA) rating, which reduces the loss in the coils; and to make the primary side resonant to reduce the power electronics converter VA rating, which reduces the loss in the power converter. Therefore, we transfer power at the magnetic resonance.

With the above analysis, we can calculate the power transfer efficiency between the two coils at the resonant frequency.

We have

$$U_{12} = I_2(R_2 + R_{Le}) = \omega M I_1 = \omega k L_1 L_2 I_1 \quad (10)$$

where R_2 is the secondary winding resistance and $R_{Le}$is the equivalent load resistance.

By defining the quality factor of the two coils, $Q_1 = \omega L_1/R_1$, $Q_2 = \omega L_2/R_2$, the transferred efficiency can be expressed as

$$\eta = \frac{I_2^2 R_{Le}}{I_1^2 R_1 + I_2^2 R_2 + I_2^2 R_{Le}} = \frac{\omega^2 k^2 Q_1 Q_2 R_2 R_{Le}}{\omega^2 k^2 Q_1 Q_2 R_2 + R_2 R_{Le} + R_{Le}^2} \quad (11)$$

By defining $a = R_{Le}/R_2$, we obtain the expression of efficiency as a function of a

$$\eta(a) = \frac{1}{\frac{1}{k^2 Q_1 Q_2} + \frac{1}{a} + a} \quad (12)$$

The maximum efficiency is obtained by solving the following equations:

$$\frac{\partial}{\partial a}\eta(a) = 0, \quad \frac{\partial^2}{\partial^2 a}\eta(a) < 0 \quad (13)$$

The maximum efficiency

$$\eta_{max} = \frac{k^2 Q_1 Q_2}{1 + \sqrt{1 + k^2 Q_1 Q_2}^2}$$

is achieved at $a_{\eta max} = 1 + k^2 Q_1 Q_2^{1/2}$.

In [64], the maximum efficiency is also derived based on several different kinds of compensation network. The results are identical and accord with the above results. The analysis here does not specify a particular compensation form. It can be regarded as a general formula to evaluate the coil performance and estimate the highest possible power transfer efficiency.

In EV wireless charging applications, the battery is usually connected to the coil through a diode-bridge rectifier. Most of the time, there is some reactive power required. The reactive power can be provide by either the coil or the compensation network like a unit-power-factor pickup. The battery could be equivalent to a resistance $R_b = U_b/I_b$, where $U_b$and $I_b$is the battery voltage and current, respectively. If the battery is connected to the rectifier directly in a seriesseries compensation form, the equivalent ac side resistance could be calculated by $R_{ac} = 8/\pi^2 \cdot R_b$. Thus, a battery load could be converted to a resistive load. The R_{ac}equation is different for different battery connection style, like with or without dc/dc converter, parallel or series compensation. Most of the time, the equivalent R_{ac}could be derived. Some typical equivalent impendence at the primary side is given in paper [42]. By calculating the equivalent ac resistances, the above equations could also be applied to a battery load with rectifier.

For stationary EV wireless charging, the coupling between the two coils is usually around 0.2. If both the sending and receiving coils have a quality factor of 300, the theoretical maximum power transfer efficiency is about 96.7%. More efficiency calculations under different coupling and quality factors are shown in Fig. 3.

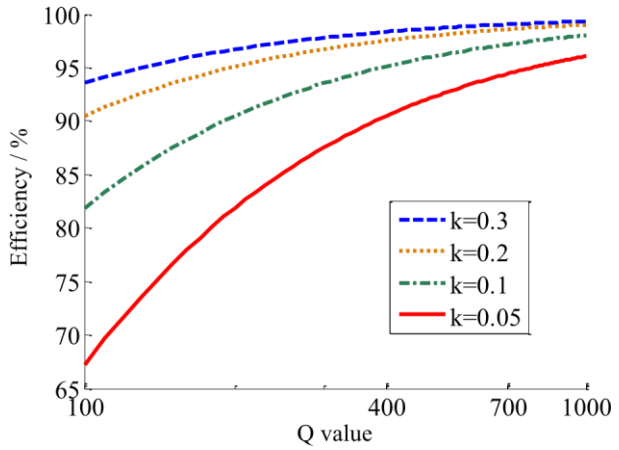

Fig. 3. Theoretical maximum transfer efficiency between two coils.

III. MAGNETIC COUPLER DESIGN

To transfer power wirelessly, there are at least two magnetic couplers in a WPT system. One is at the sending side, named primary coupler. The other is at the receiving side, named pickup coupler. Depending on the application scenarios, the magnetic coupler in a WPT for an EV could be either a pad or a track form. For higher efficiency, it is important to have high coupling coefficient k and quality factor Q. Generally, for a given structure, the larger the size to gap ratio of the coupler is, the higher the k is; the thicker the wire and the larger the ferrite section area is, the higher the Q is. By increasing the dimensions and materials, higher efficiency can be achieved. But this is not a good engineering approach. It is preferred to have higher k and Q with the minimum dimensions and cost. Since Q equals $\omega L/R$, high frequency is usually adopted to increase the value of Q. The researchers at Massachusetts Institute of Technology (MIT) used a frequency at around 10 MHz and the coil Q value reached nearly 1000 [3]. In high power EV WPT applications, the frequency is also increased to have these benefits. In Bolger's early design, the frequency is only 180 Hz [13]. A few years later, a 400 Hz frequency EV WPT system was designed by System Control Technology [14]. Neither 180 Hz

nor 400 Hz is high enough for a loosely coupled system. Huge couplers were employed in the two designs. Modern WPT system uses at least 10 kHz frequency [15]. As the technical progress of power electronics, 100 kHz could be achieved [65] at high power level. The WiTricity Company with the technology from MIT adopts 145 kHz in their design. In the recent researches and applications, the frequency adopted in an EV WPT system is between 20 and 150 kHz to balance the efficiency and cost. At this frequency, to reduce the ac loss of copper coils, Litz wire is usually adopted.

Besides the frequency, the coupling coefficient k is significantly affected by the design of the magnetic couplers, which is considered one of the most important factors in a WPT system. With similar dimensions and materials, different coupler geometry and configuration will have a significant difference of coupling coefficient. A better coupler design may lead to a 50%–100% improvement compared with some nonoptimal designs [48].

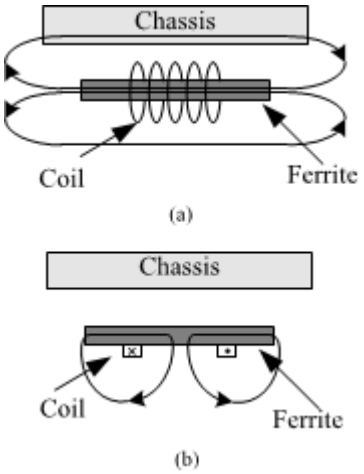

Fig. 4. Main flux path of double-sided and single-sided coupler. (a) Doublesided type. (b) Single-sided type.

A. Coupler in the Stationary Charging

In a stationary charging, the coupler is usually designed in a pad form. The very early couplers are just like a simple split core transformer [19], [38], [56]. Usually this kind of design could only transfer power through a very small gap. To meet the requirements for EV charging, the deformations from spilt core transformers and new magnetic coupler forms are presented for large gap power transfer [12], [31], [37], [42], [47]–[50], [66]–[71]. According to the magnetic flux distribution area, the coupler could be classified as the double-sided and single-sided types. For the double-sided type, the flux goes to both sides of the coupler [12], [31], [67]. A flattened solenoid inductor form is proposed in [12] and [67]. Because the flux goes through the ferrite like through a pipe, it is also called a fluxpipe coupler. To prevent the eddy current loss in the EV chassis, an aluminum shielding is usually added which bring a loss of 1%–2% [12]. When the shielding is added, the quality factor of a flux-pipe coupler reduces from 260 to 86 [48]. The high shielding loss makes the double-sided coupler not the optimal choice. For the single-sided coupler, most of the flux exists at only one side of the coupler. As shown in Fig. 4, the main flux path flows through the ferrite in a single-sided coupler. Unlike the double-sided coupler having half of the main flux at the back, the single-sided coupler only has a leakage flux in the back. This makes the shielding effort of a single-sided type much less.

Two typical single-sided flux type pads are shown in Fig. 5. One is a circular unipolar pad [47]. Another one is a rectangular bipolar pad proposed by University of Auckland, which is also named DD pad [48]. Besides the mechanical support material, a single-sided pad is composed of three layers. The top layer is the coil. Below the coil, a ferrite layer is inserted for the purpose of enhancing and guiding the flux. At the bottom is a shielding layer. To transfer power, the two pads are put closed with coil to coil. With the shielding layer, most of the high-frequency alternating magnetic flux can be confined in the space between the two pads. A fundamental flux path concept was proposed in the flux pipe paper [67].

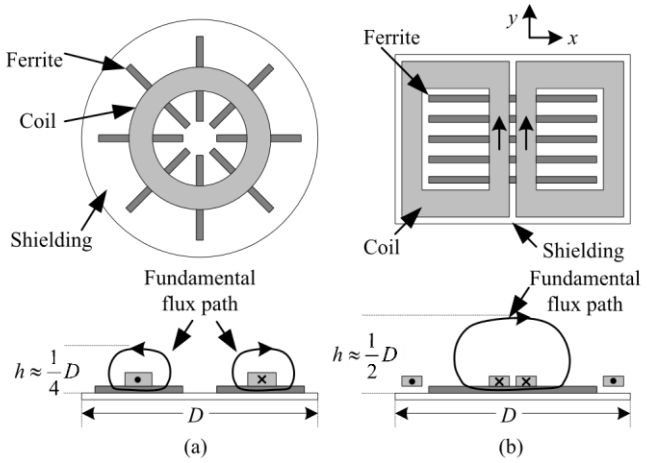

Fig. 5. Two typical single-sided flux type pads. (a) Circular pad. (b) DD pad.

The flux path height of a circular pad is about one-fourth of the pad's diameter. While for a DD pad, the height is about half of the pad's length. For a similar size, a DD pad has a significant improvement in the coupling. The charge zone for a DD pad could be about two times larger than a circular pad with similar material cost. The DD pad has a good tolerant in the y-direction. This makes the DD pad a potential solution for the dynamic charging when the driving direction is along with the y-axis. However, there is a null point for DD pad in the x-direction at about 34% misalignment [48]. To increase

the tolerant in *x*-direction, an additional quadrature coil named Q coil is proposed to work together with the DD pad, which is called DDQ pad [48], [49], [68]. With a DDQ receiving pad on a DD sending pad, the charge zone is increased to five times larger than the circular configuration. As the additional Q coil in the receiver side, the DDQ over DD configuration uses almost two times copper compared with the circular one [48]. A variant of a DDQ pad, which is called a new bipolar pad, was also proposed by University of Auckland [49], [50]. By increasing the size of each D pad and having some overlap between the two D coils, the new bipolar pad could have a similar performance of a DDQ pad with 25% less copper. With all the efforts, at 200 mm gap, the coupling between the primary and secondary pads could achieve 0.15–0.3 with an acceptable size for an EV. Referred to Fig. 3, at this coupling level, efficiency above 90% could possibly be achieved.

B. Coupler in the Dynamic Charging

The dynamic charging, also called the OLEVs [56] or roadway powered electric vehicles [14], is a way to charge the EV while driving. It is believed that the dynamic charging can solve the EVs' range anxiety, which is the main reason limits the market penetration of EVs. In a dynamic charging system, the magnetic components are composed of a primary side magnetic coupler, which is usually buried under the road, and a secondary side pickup coil, which is mounted under an EV chassis. There are mainly two kinds of primary magnetic coupler in the dynamic charging. The first kind is a long track coupler [26], [31], [57], [70], [72]–[76]. When an EV with a

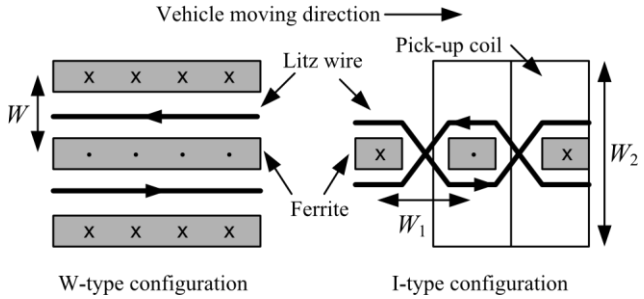

Fig. 6. Top view of W-shape and I-shape track configuration.

pickup coil is running along with the track, continues power can be transferred. The track can be as simple as just two wires [37], [77], or an adoption of ferrites with U-type or W-type [26], [56] to increase the coupling and power transfer distance. Further, a narrow-width track design with an I-type ferrite was proposed by KAIST [72], [73]. The differences between the W-type and I-type are shown in Fig. 6. For W-type configuration, the distribution area of the ferrite W determines the power transfer distance, as well as the lateral displacement. The total width of W-type should be about four times the gap between the track and the pickup coil. For I-type configuration, the magnetic pole alternates along with the road. The pole distance W_1 is optimized to achieve better coupling at the required distance. The width of pickup coil W_2 is designed to meet the lateral misalignment requirement. The relation between track width and transfer distance is decoupled and the track can be built at a very narrow form. The width for U-type and W-type is 140 and 80 cm, respectively [73]. For I-type, it could be reduced to only 10 cm with a similar power transfer distance and misalignment capacity. 35 kW power was transferred at a 200 mm gap and 240 mm displacement using the I-type configuration [73]. With the narrowed design, the construction cost could be reduced. Also, the track is far away from the road side, the electromagnetic field strength exposed to pedestrians can also be reduced.

The problem of the track design is that the pickup coil only covers a small portion of the track, which makes the coupling coefficient very small. The poor coupling brings efficiency and electromagnetic interference (EMI) issues. To reduce the EMI issue, the track is built by segments [52], [70], [75] with a single power converter and a set of switches to power the track. The excitation of each segment can be controlled by the switches' ON-OFF state. The electromagnetic field above the inactive segments is reduced significantly. However, there is always a high-frequency current flowing through the common supply cables, which lowers the system efficiency. The published systems efficiency is about 70%–80%, which is much lower than the efficiency achieved in the stationary charging.

When each segment is short enough, the track becomes like a pad in the stationary charging, which is the other kind of the primary magnetic coupler. Each pad can be driven by an independent power converter. Thus, the primary pads can be selectively excited without a high-frequency common current. Also, the energized primary pad is covered by the vehicle. The electromagnetic field is shielded to have a minimum impact

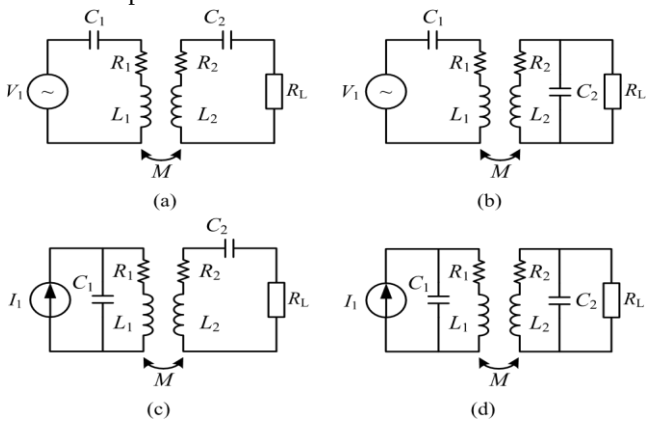

Fig. 7. Four basic compensation topologies. (a) SS. (b) SP. (c) PS. (d) PP.

to the surrounding environment. The efficiency and EMI performance could be as good as that in a stationary charging application. However, the cost to build a power converter for each pad is unaffordable. It is desired to use only one converter to drive a few pads, and the current in each pad can be controlled. A double-coupled method was proposed with each pad configured with an intermediary coupler and a bidirectional switch [78]. The intermediary couplers are coupled to one primary coil at the converter side. The intermediary coupler performs like a high-frequency current source. By controlling the ON-OFF time of the switch, the current in each pad can be controlled. However, even the corresponding pad is shut down by the switches, the high-frequency current is always circulating in all the intermediary couplers, which may lower the efficiency. A reflexive field containment idea by North Carolina State University was also proposed [79]. Three pads are driven from only one power converter. By carefully designing the primary and pickup parameters, the reflexive field of the pickup pad could enhance the current in the primary pad. The current in each primary pad is sensitive to the coupling condition and could be automatically built up when the pickup pad is coupled. The current decreases very quickly when the pickup pad moves away. The relation between the primary pad current and coupling coefficient is carefully designed. For dynamic charging, the EV runs freely on the road which makes the coupling varies in a wide range. To make this method more practical, the system characteristics under coupling variation caused by the lateral misalignment, vehicle forward movement and vehicle types should be studied further.

IV. COMPENSATION NETWORK

In a WPT system, the pads are loosely coupled with a large leakage inductance. From the analysis in Section II, it is required to use a compensation network to reduce the VA rating in the coil and power supply. In early inductive charging designs, the compensation is set on primary or secondary side only [18]. When the coupling coefficient is reduced to less than 0.3 in the EV WPT, compensation at both the primary and secondary side is recommended to have a more flexible and advanced characteristics. To compensate a

TABLE I PRIMARY COMPENSATION CAPACITANCE

Topology	Primary Capacitance C_1
SS	$\frac{C_2 L_2}{L_1}$
SP	$\frac{C_2 L_2}{L_1} \cdot \frac{1}{1-k^2}$
PS	$\frac{C_2 L_2}{L_1} \cdot \frac{1}{Q_s^2 k^4 + 1}$
PP	$\frac{C_2 L_2}{L_1} \cdot \frac{1-k^2}{Q_s^2 k^4 + (1-k^2)^2}$

leakage inductance, the simplest way is to add a capacitor at each side. As shown in Fig. 7, depending on how the capacitors are connected to the coils, there are four basic compensation topologies, which are series-series (SS), series-parallel (SP), parallel-parallel (PP), and parallel-series (PS) [21], [23], [27], [80]–[82]. If the primary is series compensated, a voltage source converter could be connected directly to the coil. If the primary is parallel compensated, usually an inductor is inserted to change the converter to a current source. The secondary side capacitor C_2 is usually designed to resonant with L_2 to reduce the VA capacity of the coils. When the primary side coil has a constant current, a series compensation at the secondary side makes the output like a voltage source, while a parallel compensation makes the output like a current source [27]. However, not all the design has a constant primary side current, and different output characteristics can exist for a series or parallel compensation at the secondary side.

To reduce the power converter VA rating, the primary side capacitor is usually tuned to make the input voltage and current in phase at certain coupling and load condition, which is called the zero-phase-angle (ZPA) method. To realize softswitching for power electronics converters, the primary side compensation network is often tuned to make the primary side has a small portion of reactive power to reach zero voltage switching (ZVS) or zero current switching (ZCS) condition [22], [44], [83]. Since the tuned reactive power is relative small, the parameters for realizing ZVS and ZCS are close to the parameters designed by ZPA method.

To calculate the primary side capacitance, a secondary load quality factor is defined. For series compensated secondary, $Q_s = \omega_0 L_2/R_L$. For parallel-compensated secondary, $Q_s = R_L/\omega_0 L_2$, where ω_0 is the resonant frequency. The load quality factor is a ratio between the reactive and active power. To achieve ZPA at the primary side, the primary capacitances for different types are listed in Table I [27]. From Table I, we can see the primary compensation capacitance is a constant value for SS method regardless of the coupling and load conditions. For SP method,

the capacitance varies when the coupling changes. For PS and PP, the capacitance is affected by both the coupling and load conditions.

When the secondary is at resonant frequency, the reflected load at the primary side could be calculated

$$Rr\_ss = Rr\_ps = \frac{\omega_0 2M2}{RL} \quad (14)$$

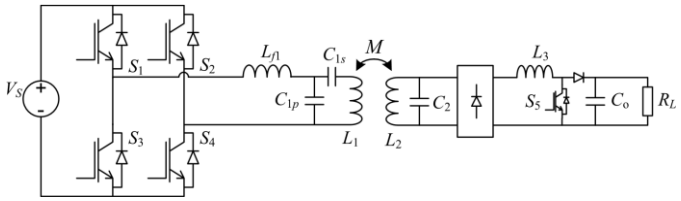

Fig. 8. Circuit schematic of a typical WPT configuration.

$$Rr\_sp = Rr\_pp = \frac{M2\ RL}{L2^2}. \quad (15)$$

For SS structure, from (14) we see that when the coupling reduces, the reflected resistance at the primary side reduces. This will increase the output power when the primary side is connected to a voltage source. For PS structure, the reflected resistance changes in the same way as the change of coupling. However, the PS structure should be connected to a current source. The output power will reduce when the coupling reduces. To maintain a constant output power when the coupling changes, SPS compensation method was proposed in [84]. It can be regarded as a combination of SS and PS. By designing a proper ratio between the two primary side capacitors, the characteristic of SS and PS are mixed. Thus, constant output power is achieved at a high misalignment tolerant without adjusting the primary power supply.

By introducing a inductor-capacitor (LC) compensation network, a primary side inductor-cap (LCL) current source structure is widely used in the inductive heating and wireless power transfer applications [44], [85]–[88]. The advantage of the LCL structure is obvious. At the resonant frequency, a LCL network performs like a current source. The current in the primary side coil is controlled by the high-frequency square wave voltage from the power converter regardless of the coupling and load condition. This makes the control at the primary side much easier. Moreover, by tuning the LCL parameters, the reactive power can be fully compensated. The power converter provides the active power only. The required VA rating for the power converter can also be minimized.

Together with the LCL primary compensation, compensation using parallel form at the secondary is adopted in many designs [55], [69]. The power control and decoupling method for a parallel structure has been well developed [21]. However, a parallel-compensated system has a large reactive current in the pickup coil and the reactive power is reflected to the primary side. To overcome the disadvantage of the parallel pick compensation, a unit power factor pickup is proposed by University of Auckland [89]–[91]. By introducing a LCL form pickup coil, the circulating current in the pickup coil can be minimized and only the active load is reflected to the primary side. To cancel the nonlinear effect of the rectifier diodes, another capacitor is introduce to form a LCLC compensation form, which could achieve an exactly unit power factor at predetermined load condition. From the comparisons, the difference of a LCL and LCLC form is insignificant.

Both of the LCL and LCLC structure achieve a significant efficiency improvement compared with the traditional LC parallel structure.

V. POWER ELECTRONICS CONVERTER AND POWER CONTROL

In a WPT system, the function of the primary side power electronics converter is to generate a high-frequency current in the sending coil. To increase the switching frequency and efficiency, usually a resonant topology is adopted [21]–[23], [55], [85], [87], [88],[92]–[96]. At the secondary side, a rectifier is adopted to convert the high-frequency ac current to dc current. Depending on whether a secondary side control is needed, an additional converter may be employed. The primary side converter may be a voltage or a current source converter. As a bulky inductor is needed for the current source converter, the most common choice at the primary side is a full bridge voltage source resonant converter. A typical wireless power circuit schematic is shown in Fig. 8. In the primary side, the full bridge converter outputs a high-frequency square voltage. By adopting the LC compensation network, a constant highfrequency current can be maintained in L_1. An additional capacitor C_{1s} is introduced here to compensated part of the reactive power on L_1. Thus, the power rating on L_{f1} could be reduced. The system design flexibility could also be improved. At the secondary side, the parallel compensation is adopted. With a constant primary coil current and parallel secondary side compensation, the output is like a current source. At a certain coupling, the current in L_3 is almost constant. By changing the duty ratio of switch S_5, the output power can be controlled.

Many different control methods were proposed to control the transferred power. Depending on where the control

action is applied, the control method could be classified as primary side control [92], [95], [97], secondary side control [27], [30], [45], and dual-side control [55]. In most cases, the primary side and dual-side control is only suitable for power transfer from one primary pad to one pickup pad. The secondary side control could be used in the scenario where multiple pickup pads are powered from one primary pad or track.

The control at the primary side can be realized by changing the frequency, duty cycle and the phase between the two legs. Since the characteristic of a resonant converter is related to the operating frequency, a frequency control at the primary side is adopted in some designs [53], [98]. When adjusting the frequency, it should be noted that the bifurcation phenomenon in the loosely coupled systems [23]. The power versus frequency is not always a monotonic function. Also, the frequency control method takes up a wider radio frequency bandwidth, which may increases the risk of electromagnetic interference. When the switching frequency is fixed, the control can be carried out by duty cycle or phase shift [99]. The problem of duty cycle or phase shift control is that there is a high circulating current in the converter. Also, the ZVS or ZCS switching condition may be lost. To ensure ZVS, an alternative way to control the system output power is to adjust the input dc voltage V_S [73]. An asymmetrical voltage cancellation method, which uses an alternative way to change the duty cycle, was proposed to increase the ZVS region [88]. A discrete energy injection method, which could achieve ZCS and lower the switching frequency at light load condition, was proposed in [43], [92], and [94].

At the secondary side, as shown in Fig. 8, with parallel compensation, a boost converter is inserted after the rectifier for the control. Correspondingly, with series compensation, a buck converter can be used. When the control is after the rectifier, an additional dc inductor, as well as a diode on the current flow path, should be introduced. The University of Auckland proposed a control method at the ac side before the rectifier. By doing so, the dc inductor and additional diodes could be saved. Because of the resonating in the ac side, ZVS and ZCS could be achieved. The detailed designs for series compensation as well as a LC compensation network are presented in [91], [100], and [101]. The dual-side control is a combination of both primary and secondary side control [55]. The system complexity and cost may increase, but the efficiency can be optimized by a dual-side control.

VI. STUDY METHODS

WPT involves multiple disciplines, including magnetics, power electronics, communications, mechanical engineering, and electric engineering. The study of a WPT system can be very complex owing to the multidisciplinary nature and the uncertainties of the system. For example, the magnetic field is at high frequency and low density, and varies with gap distance, misalignment, and power levels. The resonance in the system is key to the high efficiency power transfer but that could be also affected by coupling between the two coils, and surrounding media (raining or dry environment). Typically, the study of WPT systems involves:

1) analytical method, including circuit analysis and calculation of mutual inductances through analytical approaches;
2) field analysis using numerical tools such as finite element methods, finite boundary method, highfrequency structured system analysis, and so forth;
3) simulation of lumped model involving parametric analysis, that is, coupling coefficient change versus efficiency, and so forth;
4) experimental study involving the use network analyzers and field measurements and parameter identifications of the WPT system and its resonant characteristics;

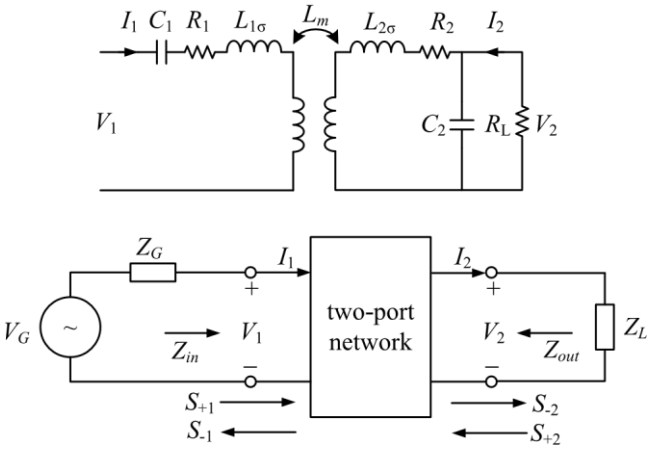

Fig. 9. WPT system with SP resonant topology and its representation as a two-port network. Top: SP topology. Bottom: two-port network of a WPT system.

5) soft switching of the power converters in a WPT system that involve the various methods to study power electronic circuits.

In particular, two-port network theory can be an efficient tool for the study of WPT systems [102]. Fig. 9 shows the WPT system with SP resonant topology and its generic two-port network representation.

The impedance matrix, transfer matrix, and scattering matrix can be defined as Impedance matrix-Z

$$V1 \quad Z11\ V2 = Z21 \quad Z12\ I1$$

Transfering matrix-T

$$Z22$$

$$-I2$$

$$V_1 \quad a\ I1 = c \quad b\ V_2$$

Scattering matrix-S

$$= Z0\ (1 + S11)(1 - S22) + S12S21 \quad 2S12 \quad d$$

$$Z$$

$$DS \quad 2S21 \quad (1 - S11)(1 + S22) + S12S21 \quad -I_2$$

$$= \quad 1\ (Z11 - Z0)(Z22 + Z0) - Z12Z21 \quad 2Z12Z0$$

$$S$$

$$DZ \quad 2Z21Z0 \quad (Z11 + Z0)(Z22 - Z0) - Z12Z21$$

$$S12\ a1$$

.

$$S22$$

$$b1\ S11\ b2 = S21 \quad a2$$

By rearrange the equations above, we can obtain the relationships between impedance matrix and the transfer matrix

$$3) = 1\ a \quad -(ad - bc)c \quad 1 \quad -d$$

$$Z$$

$$= 1\ Z11 - (Z11Z22 - Z12Z21)T \quad .$$

$$Z21 \quad 1 \quad -Z_{22}.$$

Similarly, we can obtain the relationships between impedance matrix and the scattering matrix as shown at the top of next page.

where

$DZ = (Z11 + Z0)(Z22 + Z0) - Z12Z21$ $DS = (1 - S11)(1 - S22) - S12S21.$

Input power to the network

$$|VS|2 = |VS|2\ (1 - ||-\text{in}|2)|1 - |\ S|2$$

$$P1 = |Z + Z\ |2\ R\text{in}4Z0 \quad 1 \quad \text{in}S2 \quad .$$

$$S \quad \text{in}$$

Output power

$$= \quad | \quad +|Z21|2|VS|2 \quad |$$

$$P2 \quad (Z\text{in} \quad ZS)(Z22 + ZL)\ 2\ RL$$

$$= |VS|2 \quad (1 - |L|2)|1 - S|2|S21|2 \quad |$$

.

$$4Z0\ |(1 - S11S)(1 - S22L) - S12S21SL\ 2$$

Efficiency

$$\eta = P2 = - |1 \quad | \quad 1 - |L|2 \quad | \quad |2$$

$$2\ |1 - |S22L|2\ S21$$

$$P1 \quad 1 \quad \text{in}$$

where $_{\text{in}}$ is the input reflection coefficient, $_L$ is the load reflection coefficient, and Z_{in} is the input impedance.

For SP topology, we can derive the transfer parameters as follows:

$$1 \quad 1 \quad L2C2$$

$$4) \quad a = \_\_L_m \quad L1 - \_\_\_\_\omega 2C1 + R1C2$$

$$R2 + \quad \_\_\_\_C1$$

$$+ \_\_1 - \omega 2C2L1L2 - L2m + \quad j - R1 \_\_$$

$$Lm \quad Lm \quad \omega$$

$$+ \_\_ \quad j\ \omega C2R2L1 - C2R2 + \omega C2\ R1L2$$

$$Lm \quad \omega C1\ 1 \quad R_2 \quad b = \quad L^1R2 - \quad 2_C1 + R^1L2$$

$$_Lm \quad \omega$$

$$+ \quad \_\_ \quad \_\_\_\_ \quad j \quad - R1R2 + \omega L1L2 - L2m -$$

$$\_\_\_\_L2$$

$$5) \quad L_m \quad \omega \quad \omega C_1$$

$$c = \quad 1\ C\ R + \ -1 + \omega_C 2_L 2$$

$$2 \quad 2 \quad _j$$

$$L_m \quad \omega\ d = \quad 1\ L_2 + j \ - R2\ .$$

$$6) \quad \_\_ \quad L_m \quad \omega \_\_$$

From the above equations, one can easily study the system performance by adjusting the parameters of the system.

VII. ADDITIONAL DISCUSSION

A. Safety Concerns

WPT avoids the electrocution danger from the traditional contact charging method. But, when charging an EV battery wirelessly, there is a high-frequency magnetic field existing between the transmitting and receiving coils. The magnetic flux coupled between the two coils is the foundation for WPT, which cannot be shielded. The large air-gap between the two coils causes a high leakage field. The frequency and amplitude of the leakage magnetic field should be elaborately controlled to meet the safety regulations.

A safe region should always be defined for a wireless charging EV. We should ensure that the magnetic flux density should meet the safety guidelines when people are in normal positions, such as standing outside a car or sitting inside a car. Fortunately, a car is usually made of steel, which is a very good shielding material.

The guideline published by the International Commission on Non-Ionizing Radiation Protection (ICNIRP) is the most referenced standard to ensure the human safety. There are two versions of ICNIRP standards. The first one was published at 1998. In ICNIRP 1998, there are two reference levels for occupational and general public exposure, respectively. At frequency 0.8–150 kHz, which covers most of the EV WPT frequency, the limit for general public exposure is 6.25 μT.

For occupational exposure, it is a little different. At frequency 0.82–65 kHz, the limit is 30.7 μT. While at 0.065–1 MHz, the limit is 2/*f* .*f* is the frequency measured in MHz. Under the ICNIRP 1998 guideline, the safety evaluation for a 5 kW stationary EV WPT system was conducted [55]. The average magnetic field exposed to a 1500 mm height body was 4.36 μT. For a 35 kW dynamic EV WPT system, the magnetic flux density at 1 m from the center of the road is 2.8 μT [72]. Both the stationary and dynamic WPT system design could meet the ICNIRP 1998 safety guidelines. A good thing for EV WPT is that, after another 10 years of experience on the health affection of time-varying electromagnetic, ICNIRP revised the guideline at 2010 and increased the reference level significantly. For occupational exposure, the reference level is relaxed to 100 μT. For general public, the value changes from 6.25 to 27 μT. The increase in the reference level is because the former guideline is too conservative. There is another standard about the electromagnetic field safety issues, IEEE Std. C95.1-2005, presented by the IEEE International Committee on Electromagnetic Safety. In IEEE Std. C95.1-2005, the maximum permissible exposure of head and torso is 205 μT for general public, and 615 μT for occupation. The maximum permissible exposure for the limbs is even higher, which is 1130 μT for both the general public and occupation. Compared with the IEEE Std., the ICNIRP 2010 standard is still conservative. According to ICNIRP 2010, the exposure safety boundaries of our 8 kW EV WPT system for both occupation and general public people are shown in Fig. 10. Together with the chassis, the safety zone is quite satisfactory. On the premise of safety, higher power WPT system could be developed according to the ICNIRP 2010.

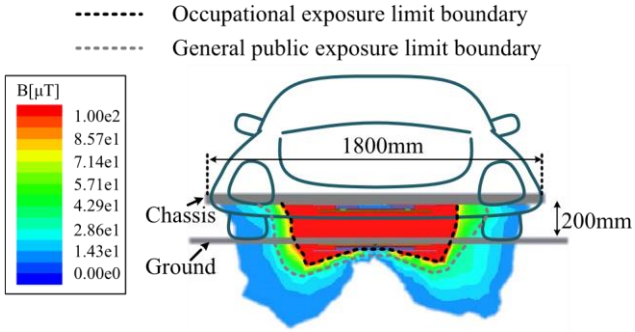

Fig. 10. Exposure limit boundary for an 8 kW WPT system.

Besides the safety issue, the emission limit for Industrial, Scientific, and Medical (ISM) equipment is also regulated by Federal Communications Commission (FCC) in Title 47 of the Code of Federal Regulations (CFR 47) in part 18 in United States. According to FCC part 18, ISM equipment operating in a specified ISM frequency band is permitted unlimited radiated energy. However, the lowest ISM frequency is at 6.78 MHz, which is too high for EV WPT. When the WPT operates at a non-ISM frequency, the field strength limit should be subjected to §18.305. The Society of Automotive Engineers (SAE) has already formed a committee, J2954, to look into many issues related to EV WPT systems. Among one of their goals will be safety standards. It is projected that a SAE standard on EV WPT systems will be released in June 2014 by this committee. More standards and regulations from different regions are summarized in a paper from Qualcomm Incorporated [103].

B. Vehicle to Grid Benefits

As the ongoing develop of EV, the vehicle to grid (V2G) concept, which studies the interaction between mass EV charging and the power grid, is also a hot research topic in smart grid and EV areas. It is recognized that if the EV charging procedure could be optimized, it could have many benefits for the grid. The EV could balance the loads by valley filling and peak shaving. The batteries in the EVs are like an energy bank, thus some unstable new energy power supply, like wind power, could be connected to the grid more easily. When the secondary rectifier diodes are replaced by active switches, a bidirectional WPT function is realized [104]–[112]. The bidirectional WPT could provide advanced performance in V2G applications. Studies show that by introducing WPT technology, the drivers are more willing to connect their EV into the grid [113], which could maximize the V2G benefits.

C. Wireless Communications

In a WPT system, it is important to exchange information between the grid side and vehicle side wirelessly to provide a feedback. Thus, the power flow could be controlled by the methods mentioned in Section V. The communication design could be classified by whether the signal is modulated on the power carrier or uses a separate frequency band.

The Qi standard for wireless low-power transfer modulates a 2 kHz signal onto the power carrier frequency [114]. The communication signal is transmitted through the power coils. The 2 kHz signal is very easy to process even by using the existing microcontroller in the device. In this way, the extra antennas and control chips for the communication could be saved. In EV WPT system, for the high voltage on the power coils, isolation is required for the communication control circuit which may increase the cost. For advanced information exchange, general wireless communication protocols, like Bluetooth, near field communication (NFC), and so on, could be adopted. In the EV WPT prototype from ORNL, the Dedicated Short Range Communications (DSRC) Link is used [95]. The DSRC is a technology based on global

position system and IEEE 802.11p wireless fidelity (Wi-Fi), which could realize the connection between vehicle-to-vehicle (V2V) and vehicle-to-infrastructure (V2I) [115]. The FCC already allocates 75 MHz band at 5.9 GHz for DSRC. It is being committed to use by the U.S. Department of Transportation in the Intelligent Transportation System. As the IEEE and SAE standards were already published, the DSRC could provide an easier way to implement the smart grid functionalities and maximize the vehicle to grid benefits.

D. Cost

An importance factor that affects the future of WPT is its cost. Actually, from Fig. 8 we see the WPT has only a little difference with a wired charger. The extra cost in a WPT is mainly brought by the magnetic coupler. For our 8 kW stationary WPT design [61], the material cost of the two magnetic couplers is about $400. This will be the rough cost increase of an 8 kW wireless charger compared with a wired charger, which is quite acceptable if considering all the convenience brought by the WPT and long-term operation cost savings and reduction of battery size. For the dynamic WPT design, the infrastructure cost including converter and track for 1km oneway road is controlled to $0.4 million [57]. The investment of electrification is much lower with the construction cost of the road itself. With the road electrification, the EV on-board batteries could be reduced to 20%. The savings on the batteries might be much more than the investment on the infrastructure. Studies also show that with only 1% electrification of the urban road, most of the vehicles could meet a 300-mile range easily [60], [116]. The road electrification time is coming.

VIII. CONCLUSION

This paper presented a review of wireless charging of electric vehicles. It is clear that vehicle electrification is unavoidable because of environment and energy related issues. Wireless charging will provide many benefits as compared with wired charging. In particular, when the roads are electrified with wireless charging capability, it will provide the foundation for mass market penetration for EV regardless of battery technology. With technology development, wireless charging of EV can be brought to fruition. Further studies in topology, control, inverter design, and human safety are still needed in the near term.

REFERENCES

[1] S. J. Gerssen-Gondelach and A. P. C. Faaij, "Performance of batteries for electric vehicles on short and longer term," *J. Power Sour.*, vol. 212, pp. 111–129, Aug. 2012.

[2] V. Etacheri, R. Marom, R. Elazari, G. Salitra, and D. Aurbach, "Challenges in the development of advanced Li-ion batteries: A review," *Energy Environ. Sci.*, vol. 4, no. 9, pp. 3243–3262, 2011.

[3] A. K. A. Kurs, R. Moffatt, J. D. Joannopoulos, P. Fisher, and M. Soljacic, "Wireless power transfer via strongly coupled magnetic resonances," *Science*, vol. 317, no. 5834, pp. 83–86, 2007.

[4] P. Sample, D. A. Meyer, and J. R. Smith, "Analysis, experimental results, and range adaptation of magnetically coupled resonators for wireless power transfer," *IEEE Trans. Ind. Electron.*, vol. 58, no. 2, pp. 544–554, Feb. 2011.

[5] L. Cannon, J. F. Hoburg, D. D. Stancil, and S. C. Goldstein, "Magnetic resonant coupling as a potential means for wireless power transfer to multiple small receivers," *IEEE Trans. Power Electron.*, vol. 24, no. 7, pp. 1819–1825, Jul. 2009.

[6] Kurs, R. Moffatt, and M. Soljacic, "Simultaneous mid-range power transfer to multiple devices," *Appl. Phys. Lett.*, vol. 96, no. 4, pp. 044102-1–044102-3, 2010.

[7] Sanghoon, K. Yong-Hae, S.-Y. Kang, L. Myung-Lae, L. Jong-Moo, and T. Zyung, "Circuit-model-based analysis of a wireless energytransfer system via coupled magnetic resonances," *IEEE Trans. Ind. Electron.*, vol. 58, no. 7, pp. 2906–2914, Jul. 2011.

[8] Kainan and Z. Zhengming, "Analysis of the double-layer printed spiral coil for wireless power transfer," *IEEE J. Emerg. Sel. Topics Power Electron.*, vol. 1, no. 2, pp. 114–121, Jul. 2013.

[9] Z. Yiming, Z. Zhengming, and C. Kainan, "Frequency decrease analysis of resonant wireless power transfer," *IEEE Trans. Power Electron.*, vol. 29, no. 3, pp. 1058–1063, Mar. 2014.

[10] L. C. Kwan, W. X. Zhong, and S. Y. R. Hui, "Effects of magnetic coupling of nonadjacent resonators on wireless power domino-resonator systems," *IEEE Trans. Power Electron.*, vol. 27, no. 4, pp. 1905–1916, Apr. 2012.

[11] W. X. Zhong, L. C. Kwan, and S. Y. Hui, "Wireless power dominoresonator systems with noncoaxial axes and circular structures," *IEEE Trans. Power Electron.*, vol. 27, no. 11, pp. 4750–4762, Nov. 2012.

[12] Y. Nagatsuka, N. Ehara, Y. Kaneko, S. Abe, and T. Yasuda, "Compact contactless power transfer system for electric vehicles," in *Proc. IPEC*, Jun. 2010, pp. 807–813.

[13] J. G. Bolger, F. A. Kirsten, and L. S. Ng, "Inductive power coupling for an electric highway system," in *Proc. 28th IEEE Veh. Technol. Conf.*, Mar. 1978, pp. 137–144.

[14] M. Eghtesadi, "Inductive power transfer to an electric vehicleanalytical model," in *Proc. IEEE 40th Veh. Technol. Conf.*, May 1990, pp. 100–104.

[15] A. W. Green and J. T. Boys, "10 kHz inductively coupled power transfer-concept and control," in *Proc. 5th Int. Conf. Power Electron. Variable-Speed Drives*, Oct. 1994, pp. 694–699.

[16] K. W. Klontz, D. M. Divan, D. W. Novotny, and R. D. Lorenz, "Contactless power delivery system for mining applications," *IEEE Trans. Ind. Appl.*, vol. 31, no. 1, pp. 27–35, Jan./Feb. 1995.

[17] J. M. Barnard, J. A. Ferreira, and J. D. Van Wyk, "Sliding transformers for linear contactless power delivery," *IEEE Trans. Ind. Electron.*, vol. 44, no. 6, pp. 774–779, Dec. 1997.

[18] N. H. Kutkut and K. W. Klontz, "Design considerations for power converters supplying the SAE J-1773 electric vehicle inductive coupler," in *Proc. 12th Annu. APEC and Expo.*, vol. 2. Feb. 1997, pp. 841–847.

[19] A. G. Pedder, A. D. Brown, and J. A. Skinner, "A contactless electrical energy transmission system," *IEEE Trans. Ind. Electron.*, vol. 46, no. 1, pp. 23–30, Feb. 1999.

[20] H. Abe, H. Sakamoto, and K. Harada, "A noncontact charger using a resonant converter with parallel capacitor of the secondary coil," *IEEE Trans. Ind. Electron.*, vol. 36, no. 2, pp. 444–451, Mar./Apr. 2000.

[21] J. T. Boys, G. A. Covic, and A. W. Green, "Stability and control of inductively coupled power transfer systems," *Proc. IEE Electr. Power Appl.*, vol. 147, no. 1, pp. 37–43, Jan. 2000.

[22] A. P. Hu, J. T. Boys, and G. A. Covic, "ZVS frequency analysis of a current-fed resonant converter," in *Proc. 7th IEEE Int. Power Electron. Congr.*, Oct. 2000, pp. 217–221.

[23] W. Chwei-Sen, G. A. Covic, and O. H. Stielau, "Power transfer capability and bifurcation phenomena of loosely coupled inductive power transfer systems," *IEEE Trans. Ind. Electron.*, vol. 51, no. 1, pp. 148–157, Feb. 2004.

[24] J. T. Boys, G. A. Covic, and X. Yongxiang, "DC analysis technique for inductive power transfer pick-ups," *IEEE Power Electron. Lett.*, vol. 1, no. 2, pp. 51–53, Jun. 2003.

[25] J. Hirai, K. Tae-Woong, and A. Kawamura, "Study on intelligent battery charging using inductive transmission of power and information," *IEEE Trans. Power Electron.*, vol. 15, no. 2, pp. 335–345, Mar. 2000.

[26] S. Byeong-Mun, R. Kratz, and S. Gurol, "Contactless inductive power pickup system for Maglev applications," in *Proc. Conf. Rec. Ind. Appl. Conf., 37th IAS Annu. Meeting*, vol. 3. Oct. 2002, pp. 1586–1591.

[27] W. Chwei-Sen, O. H. Stielau, and G. A. Covic, "Design considerations for a contactless electric vehicle battery charger," *IEEE Trans. Ind. Electron.*, vol. 52, no. 5, pp. 1308–1314, Oct. 2005.

[28] O. H. Stielau and G. A. Covic, "Design of loosely coupled inductive power transfer systems," in *Proc. Int. Conf. Power Syst. Technol.*, vol. 1. 2000, pp. 85–90.

[29] A. P. Hu and S. Hussmann, "Improved power flow control for contactless moving sensor applications," *IEEE Power Electron. Lett.*, vol. 2, no. 4, pp. 135–138, Dec. 2004.

[30] J. T. Boys, C. I. Chen, and G. A. Covic, "Controlling inrush currents in inductively coupled power systems," in *Proc. 7th IPEC*, vol. 2. Dec. 2005, pp. 1046–1051.

[31] G. A. J. Elliot, J. T. Boys, and G. A. Covic, "A design methodology for flat pick-up ICPT systems," in *Proc. 1st IEEE Conf. Ind. Electron. Appl.*, May 2006, pp. 1–7.

[32] A. M. Bradley, M. D. Feezor, H. Singh, and F. Y. Sorrell, "Power systems for autonomous underwater vehicles," *IEEE J. Ocean. Eng.*, vol. 26, no. 4, pp. 526–538, Oct. 2001.

[33] H. Singh *et al.*, "Docking for an autonomous ocean sampling network," *IEEE J. Ocean. Eng.*, vol. 26, no. 4, pp. 498–514, Oct. 2001.

[34] K. W. Klontz*et al.*, "Submersible contactless power delivery system," U.S. Patent 5301096, Apr. 5, 1994.

[35] W. Kyung-Il, P. H. Seok, C. Y. Hyun, and K. K. Ho, "Contactless energy transmission system for linear servo motor," *IEEE Trans. Magn.*, vol. 41, no. 5, pp. 1596–1599, May 2005.

[36] A. Esser and H. C. Skudelny, "A new approach to power supplies for robots," *IEEE Trans. Ind. Appl.*, vol. 27, no. 5, pp. 872–875, Sep./Oct. 1991.

[37] G. A. J. Elliott, G. A. Covic, D. Kacprzak, and J. T. Boys, "A new concept: Asymmetrical pick-ups for inductively coupled power transfer monorail systems," *IEEE Trans. Magn.*, vol. 42, no. 10, pp. 3389–3391, Oct. 2006.

[38] A. Kawamura, K. Ishioka, and J. Hirai, "Wireless transmission of power and information through one high-frequency resonant AC link inverter for robot manipulator applications," *IEEE Trans. Ind. Appl.*, vol. 32, no. 3, pp. 503–508, May/Jun. 1996.

[39] S. I. Adachi, F. Sato, S. Kikuchi, and H. Matsuki, "Consideration of contactless power station with selective excitation to moving robot," *IEEE Trans. Magn.*, vol. 35, no. 5, pp. 3583–3585, Sep. 1999.

[40] J. Sallan, J. L. Villa, A. Llombart, and J. F. Sanz, "Optimal design of ICPT systems applied to electric vehicle battery charge," *IEEE Trans. Ind. Electron.*, vol. 56, no. 6, pp. 2140–2149, Jun. 2009.

[41] J. L. Villa, J. Sallán, A. Llombart, and J. F. Sanz, "Design of a high frequency inductively coupled power transfer system for electric vehicle battery charge," *Appl. Energy*, vol. 86, no. 3, pp. 355–363, 2009.

[42] H. Chang-Yu, J. T. Boys, G. A. Covic, and M. Budhia, "Practical considerations for designing IPT system for EV

battery charging," in *Proc. IEEE VPPC*, Sep. 2009, pp. 402–407.

[43] L. H. Leo, H. Aiguo, and G. A. Covic, "Development of a discrete energy injection inverter for contactless power transfer," in *Proc. 3rd IEEE ICIEA*, Jun. 2008, pp. 1757–1761.

[44] T. C. Sen, S. Yue, S. Y. Gang, N. S. Kiong, and A. P. Hu, "Determining multiple steady-state ZCS operating points of a switch-mode contactless power transfer system," *IEEE Trans. Power Electron.*, vol. 24, no. 2, pp. 416–425, Feb. 2009.

[45] J. U. W. Hsu, A. P. Hu, and A. Swain, "A wireless power pickup based on directional tuning control of magnetic amplifier," *IEEE Trans. Ind. Electron.*, vol. 56, no. 7, pp. 2771–2781, Jul. 2009.

[46] A. J. Moradewicz and M. P. Kazmierkowski, "Contactless energy transfer system with FPGA-controlled resonant converter," *IEEE Trans. Ind. Electron.*, vol. 57, no. 9, pp. 3181–3190, Sep. 2010.

[47] M. Budhia, G. A. Covic, and J. T. Boys, "Design and optimization of circular magnetic structures for lumped inductive power transfer systems," *IEEE Trans. Power Electron.*, vol. 26, no. 11, pp. 3096–3108, Nov. 2011.

[48] M. Budhia, J. T. Boys, G. A. Covic, and H. Chang-Yu, "Development of a single-sided flux magnetic coupler for electric vehicle IPT charging systems," *IEEE Trans. Ind. Electron.*, vol. 60, no. 1, pp. 318–328, Jan. 2013.

[49] G. A. Covic, M. L. G. Kissin, D. Kacprzak, N. Clausen, and H. Hao, "A bipolar primary pad topology for EV stationary charging and highway power by inductive coupling," in *Proc. IEEE ECCE*, Sep. 2011, pp. 1832–1838.

[50] A. Zaheer, D. Kacprzak, and G. A. Covic, "A bipolar receiver pad in a lumped IPT system for electric vehicle charging applications," in *Proc. IEEE ECCE*, Sep. 2012, pp. 283–290.

[51] N. Shinohara, "Wireless power transmission progress for electric vehicle in Japan," in *Proc. IEEE RWS*, Jan. 2013, pp. 109–111.

[52] T. E. Stamati and P. Bauer, "On-road charging of electric vehicles," in *Proc. IEEE ITEC*, Jun. 2013, pp. 1–8.

[53] N. Puqi, J. M. Miller, O. C. Onar, and C. P. White, "A compact wireless charging system development," in *Proc. IEEE ECCE*, Sep. 2013, pp. 3629–3634.

[54] Systems Control Technology Inc., "Roadway powered electric vehicle project: Track construction and testing program phase 3D," California PATH Program, Inst. Transportation Studies, Univ. California, Berkeley, CA, USA, Tech. Rep. UCB-ITS-PRR-94-07, 1994.

[55] H. H. Wu, A. Gilchrist, K. D. Sealy, and D. Bronson, "A high efficiency 5 kW inductive charger for EVs using dual side control," *IEEE Trans. Ind. Informat.*, vol. 8, no. 3, pp. 585–595, Aug. 2012.

[56] L. Sungwoo, H. Jin, P. Changbyung, C. Nam-Sup,Gyu-Hyeoung, and R. Chun-Taek, "On-line electric vehicle using inductive power transfer system," in *Proc. IEEE ECCE*, Sep. 2010, pp. 1598–1601.

[57] H. Jin, L. Wooyoung, C. Gyu-Hyeong, L. Byunghun, andChun-Taek, "Characterization of novel inductive power transfersystemsfor on-line electric vehicles," in *Proc. 26th Annu. IEEE APEC Expo.*, Mar. 2011, pp. 1975–1979.

[58] Musavi, M. Edington, and W. Eberle, "Wireless power transfer: A survey of EV battery charging technologies," in *Proc. IEEE ECCE*, Sep. 2012, pp. 1804–1810.

[59] A. Covic and J. T. Boys, "Modern trends in inductive power transfer for transportation applications," *IEEE J. Emerg. Sel. Topics Power Electron.*, vol. 1, no. 1, pp. 28–41, Jul. 2013.

[60] S. Lukic and Z. Pantic, "Cutting the cord: Static and dynamic inductive wireless charging of electric vehicles," *IEEE Electrific. Mag.*, vol. 1, no. 1, pp. 57–64, Sep. 2013.

[61] T.-D. Nguyen, S. Li, W. Li, and C. Mi, "Feasibility study on bipolar pads for efficient wireless power chargers," in *Proc. APEC Expo.*, Fort Worth, TX, USA, 2014.

[62] S. Valtchev, B. Borges, K. Brandisky, and J. B. Klaassens, "Resonant contactless energy transfer with improved efficiency," *IEEE Trans. Power Electron.*, vol. 24, no. 3, pp. 685–699, Mar. 2009.

[63] S. Jaegue*et al.*, "Design and implementation of shaped magneticresonance-based wireless power transfer system for roadway-powered moving electric vehicles," *IEEE Trans. Ind. Electron.*, vol. 61, no. 3, pp. 1179–1192, Mar. 2014.

[64] K. V. Schuylenbergh and R. Puers, *Inductive Powering—Basic Theory and Application to Biomedical Systems*. New York, NY, USA:Springer-Verlag, 2009.

[65] R. Mecke and C. Rathge, "High frequency resonant inverter for contactless energy transmission over large air gap," in *Proc. IEEE 35th Annu. PESC*, vol. 3. Jun. 2004, pp. 1737–1743.

[66] J. T. Boys, G. A. J. Elliott, and G. A. Covic, "An appropriate magnetic coupling co-efficient for the design and comparison of ICPT pickups," *IEEE Trans. Power Electron.*, vol. 22, no. 1, pp. 333–335, Jan. 2007.

[67] M. Budhia, G. Covic, and J. Boys, "A new IPT magnetic coupler for electric vehicle charging systems," in *Proc. 36th Annu. Conf. IEEE Ind. Electron. Soc.*, Nov. 2010, pp. 2487–2492.

[68] M. Budhia, G. A. Covic, J. T. Boys, and H. Chang-Yu, "Development and evaluation of single sided flux

couplers for contactless electric vehicle charging," in *Proc. IEEE ECCE*, Sep. 2011, pp. 614–621.

[69] M. Chigira, Y. Nagatsuka, Y. Kaneko, S. Abe, T. Yasuda, andA. Suzuki, "Small-size light-weight transformer with new core structure for contactless electric vehicle power transfer system," in *Proc. IEEE ECCE*, Sep. 2011, pp. 260–266.

[70] S. Choi, J. Huh, W. Y. Lee, S. W. Lee, and C. T. Rim, "New cross-segmented power supply rails for roadway-powered electric vehicles," *IEEE Trans. Power Electron.*, vol. 28, no. 12, pp. 5832–5841, Dec. 2013.

[71] M. Kiani and M. Ghovanloo, "A figure-of-merit for designing highperformance inductive power transmission links," *IEEE Trans. Ind. Electron.*, vol. 60, no. 11, pp. 5292–5305, Nov. 2013.

[72] H. Jin, L. Sungwoo, P. Changbyung, C. Gyu-Hyeoung, and R. Chun-Taek, "High performance inductive power transfer system withnarrow rail width for on-line electric vehicles," in *Proc. IEEE ECCE*, Sep. 2010, pp. 647–651.

[73] J. Huh, S. W. Lee, W. Y. Lee, G. H. Cho, and C. T. Rim, "Narrow-width inductive power transfer system for online electrical vehicles," *IEEE Trans. Power Electron.*, vol. 26, no. 12, pp. 3666–3679, Dec. 2011.

[74] J. Y. Jae and K. Y. Dae, "System architecture and mathematical model of public transportation system utilizing wireless charging electric vehicles," in *Proc. 15th Int. IEEE Conf. ITSC*, Sep. 2012, pp. 1055–1060.

[75] J. Y. Jae, K. Y. Dae, and J. Seungmin, "Optimal design of the wireless charging electric vehicle," in *Proc. IEEE IEVC*, Mar. 2012, pp. 1–5.

[76] S. In-Soo and K. Jedok, "Electric vehicle on-road dynamic charging system with wireless power transfer technology," in *Proc. IEEE IEMDC*, May 2013, pp. 234–240.

[77] J. T. Boys and S. Nishino, "Primary inductance pathway," U.S. Patent 5619078, Apr. 8, 1997.

[78] R. Nagendra, J. T. Boys, G. A. Covic, B. S. Riar, and A. Sondhi, "Design of a double coupled IPT EV highway," in *Proc. 39th Annu. Conf. IEEE Ind. Electron. Soc.*, Nov. 2013, pp. 4606–4611.

[79] K. Lee, Z. Pantic, and S. Lukic, "Reflexive field containment in dynamic inductive power transfer systems," *IEEE Trans. Power Electron.*, vol. 9, no. 9, pp. 4592–4602, Sep. 2014.

[80] A. Khaligh and S. Dusmez, "Comprehensive topological analysis of conductive and inductive charging solutions for plug-in electric vehicles," *IEEE Trans. Veh. Technol.*, vol. 61, no. 8, pp. 3475–3489, Oct. 2012.

[81] W. Zhang, S.-C. Wong, C. K. Tse, and Q. Chen, "Analysis and comparison of secondary series- and parallel-compensated inductive power transfer systems operating for optimal efficiency and load-independent voltage-transfer ratio," *IEEE Trans. Power Electron.*, vol. 29, no. 6, pp. 2979–2990, Jun. 2014.

[82] Duan, C. Jiang, A. Taylor, and K. Bai, "Design of a zero-voltageswitching large-air-gap wireless charger with low electric stress for electric vehicles," *IET Power Electron.*, vol. 6, no. 9, pp. 1742–1750, Nov. 2013.

[83] Z. Pantic, B. Sanzhong, and S. Lukic, "ZCS *LCC*-compensated resonant inverter for inductive-power-transfer application," *IEEE Trans. Ind. Electron.*, vol. 58, no. 8, pp. 3500–3510, Aug. 2011.

[84] J. L. Villa, J. Sallan, J. F. S. Osorio, and A. Llombart, "Highmisalignment tolerant compensation topology for ICPT systems," *IEEE Trans. Ind. Electron.*, vol. 59, no. 2, pp. 945–951, Feb. 2012.

[85] S. Dieckerhoff, M. J. Ruan, and R. W. D. Doncker, "Design of an IGBTbased LCL-resonant inverter for high-frequency induction heating," in *Proc. Conf. Rec. IEEE Ind. Appl. Conf. 34th IAS Annu. Meeting*, vol. 3. Oct. 1999, pp. 2039–2045.

[86] L. Fischer and H. Doht, "An inverter system for inductive tube welding utilizing resonance transformation," in *Proc. Conf. Rec. IEEE, Ind. Appl. Soc. Annu. Meeting*, vol. 2. Oct. 1994, pp. 833–840.

[87] M. L. G. Kissin, H. Chang-Yu, G. A. Covic, and J. T. Boys, "Detection of the tuned point of a fixed-frequency LCL resonant power supply," *IEEE Trans. Power Electron.*, vol. 24, no. 4, pp. 1140–1143, Apr. 2009.

[88] B. Sharp and H. Wu, "Asymmetrical voltage-cancellation control for LCL resonant converters in inductive power transfer systems," in *Proc. 27th Annu. IEEE APEC Expo.*, Feb. 2012, pp. 661–666.

[89] N. A. Keeling, G. A. Covic, and J. T. Boys, "A unity-power-factor IPT pickup for high-power applications," *IEEE Trans. Ind. Electron.*, vol. 57, no. 2, pp. 744–751, Feb. 2010.

[90] N. Keeling, G. A. Covic, F. Hao, L. George, and J. T. Boys, "Variable tuning in LCL compensated contactless power transfer pickups," in *Proc. IEEE ECCE*, Sep. 2009, pp. 1826–1832.

[91] C. Y. Huang, J. T. Boys, and G. A. Covic, "LCL pickup circulating current controller for inductive power transfer systems," *IEEE Trans. Power Electron.*, vol. 28, no. 4, pp. 2081–2093, Apr. 2013.

[92] L. Li, A. P. Hu, G. A. Covic, and T. Chunsen, "A new primary power regulation method for contactless power transfer," in *Proc. IEEE ICIT*, Feb. 2009, pp. 1–5.

[93] L. Z. Ning, R. A. Chinga, T. Ryan, and L. Jenshan, "Design and test of a high-power high-efficiency loosely coupled planar wireless power transfer system," *IEEE Trans. Ind. Electron.*, vol. 56, no. 5, pp. 1801–1812, May 2009.

[94] L. H. Leo, A. P. Hu, and G. A. Covic, "A direct AC–AC converter for inductive power-transfer systems," *IEEE Trans. Power Electron.*, vol. 27, no. 2, pp. 661–668, Feb. 2012.

[95] M. Miller, C. P. White, O. C. Onar, and P. M. Ryan, "Grid side regulation of wireless power charging of plug-in electric vehicles," in *Proc. IEEE ECCE*, Sep. 2012, pp. 261–268.

[96] B. N. Xuan, D. M. Vilathgamuwa, and U. K. Madawala, "A matrix converter based inductive power transfer system," in *Proc. Conf. Power Energy IPEC*, Dec. 2012, pp. 509–514.

[97] Q. Wei *et al.*, "A new type of IPT system with large lateral tolerance and its circuit analysis," in *Proc. ICCVE*, Dec. 2012, pp. 311–315.

[98] S. Krishnan *et al.*, "Frequency agile resonance-based wireless charging system for electric vehicles," in *Proc. IEEE IEVC*, Mar. 2012, pp. 1–4.

[99] M. Borage, S. Tiwari, and S. Kotaiah, "Analysis and design of an LCL-T resonant converter as a constant-current power supply," *IEEE Trans. Ind. Electron.*, vol. 52, no. 6, pp. 1547–1554, Dec. 2005.

[100] H. H. Wu, J. T. Boys, and G. A. Covic, "An AC processing pickup for IPT systems," *IEEE Trans. Power Electron.*, vol. 25, no. 5, pp. 1275–1284, May 2010.

[101] H. H. Wu, G. A. Covic, J. T. Boys, and D. J. Robertson, "A seriestuned inductive-power-transfer pickup with a controllable AC-voltage output," *IEEE Trans. Power Electron.*, vol. 26, no. 1, pp. 98–109, Jan. 2011.

[102] S. J. Orfanidis. (2013). *Electromagnetic Waves and Antennas* [Online]. Available: http://eceweb1.rutgers.edu/~orfanidi/ewa/

[103] A. Grajski, R. Tseng, and C. Wheatley, "Loosely-coupled wireless power transfer: Physics, circuits, standards," in *Proc. IEEE MTT-S Int., Microwave Workshop Series Innovative Wireless Power Transmission, Technol., Syst., Appl.*, May 2012, pp. 9–14.

[104] U. K. Madawala and D. J. Thrimawithana, "Current sourced bidirectional inductive power transfer system," *IET Power Electron.*, vol. 4, no. 4, pp. 471–480, Apr. 2011.

[105] U. K. Madawala and D. J. Thrimawithana, "A bidirectional inductive power interface for electric vehicles in V2G systems," *IEEE Trans. Ind. Electron.*, vol. 58, no. 10, pp. 4789–4796, Oct. 2011.

[106] J. Thrimawithana and U. K. Madawala, "A three-phase bi-directional IPT system for contactless charging of electric vehicles," in *Proc. IEEE ISIE*, Jun. 2011, pp. 1957–1962.

[107] T. P. E. R. Joy, K. Thirugnanam, and P. Kumar, "Bidirectional contactless charging system using Li-ion battery model," in *Proc. 7th IEEE ICIIS*, Aug. 2012, pp. 1–6.

[108] J. Neath, A. K. Swain, U. K. Madawala, D. J. Thrimawithana, and D. M. Vilathgamuwa, "Controller synthesis of a bidirectional inductive power interface for electric vehicles," in *Proc. 3rd IEEE ICSET*, Sep. 2012, pp. 60–65.

[109] A. K. Swain, M. J. Neath, U. K. Madawala, and D. J. Thrimawithana, "A dynamic multivariable state-space model for bidirectional inductive power transfer systems," *IEEE Trans. Power Electron.*, vol. 27, no. 11, pp. 4772–4780, Nov. 2012.

[110] C. Tang, X. Dai, Z. Wang, Y. Su, and Y. Sun, "A bidirectional contactless power transfer system with dual-side power flow control," in *Proc. IEEE Int. Conf. Power Syst. Technol.*, Nov. 2012, pp. 1–6.

[111] D. J. Thrimawithana and U. K. Madawala, "A generalized steady-state model for bidirectional IPT systems," *IEEE Trans. Power Electron.*, vol. 28, no. 10, pp. 4681–4689, Oct. 2013.

[112] D. J. Thrimawithana, U. K. Madawala, and M. Neath, "A synchronization technique for bidirectional IPT systems," *IEEE Trans. Ind.Electron.*, vol. 60, no. 1, pp. 301–309, Jan. 2013.

[113] H. Xueliang, Q. Hao, H. Zhenchen, S. Yi, and L. Jun, "The interaction research of smart grid and EV based wireless charging," in *Proc. IEEE VPPC*, Oct. 2013, pp. 1–5.

[114] D. van Wageningen and T. Staring, "The Qi wireless power standard," in *Proc. 14th EPE/PEMC*, 2010, pp. S15-25–S15-32.

[115] J. B. Kenney, "Dedicated short-range communications (DSRC) standards in the United States," *Proc. IEEE*, vol. 99, no. 7, pp. 1162–1182, Jul. 2011.

[116] S. M. Lukic, M. Saunders, Z. Pantic, S. Hung, and J. Taiber, "Use of inductive power transfer for electric vehicles," in *Proc. IEEE Power Energy Soc. General Meeting*, Jul. 2010, pp. 1–6.

Chunting Chris Mi(S'00–A'01–M'01–SM'03–F'12) received the B.S.E.E. and M.S.E.E. degrees from NorthwesternPolytechnical University, Xi'an, China, and the Ph.D. degree from the University of Toronto, Toronto, ON, Canada, all in electrical engineering.

He was an Electrical Engineer with General Electric Canada Inc., Toronto. He is a Professor of Electrical and Computer Engineering and the Director of the newly established DOE funded GATE Center for Electric Drive Transportation at the University of Michigan, Dearborn, MI, USA. His current research interests include electric drives,

power electronics, electric machines, renewable energy systems, electrical and hybrid vehicles. He has conducted extensive research and authored more than 100 articles.

Dr. Mi was the Chair from 2008 to 2009 and the Vice Chair from 2006 to 2007 of the IEEE Southeastern Michigan Section. He was the General Chair of the 5th IEEE Vehicle Power and Propulsion Conference held in Dearborn in 2009. He is an Area Editor of the IEEE TRANSACTIONS ON VEHICULAR TECHNOLOGY and the IEEE TRANSACTIONS ON POWER ELECTRONICS–LETTERS, an Associate Editor of the IEEE TRANSACTIONS ON INDUSTRY APPLICATIONS, a Senior Editor of the IEEE VEHICULAR TECHNOLOGY MAGAZINE, a Guest Editor of the International Journal of Power Electronics, an Editorial Board Member of the International Journal of Electric and Hybrid Vehicles and IET ELECTRICAL SYSTEMS IN TRANSPORTATION, and was an Associate Editor of the Journal of Circuits, Systems, and Computers from 2007 to 2009. He was a recipient of the Distinguished Teaching Award and the Distinguished Research Award of the University of Michigan, the 2007 IEEE Region 4 Outstanding Engineer Award, the IEEE Southeastern Michigan Section Outstanding Professional Award, and the SAE Environmental Excellence in Transportation Award.